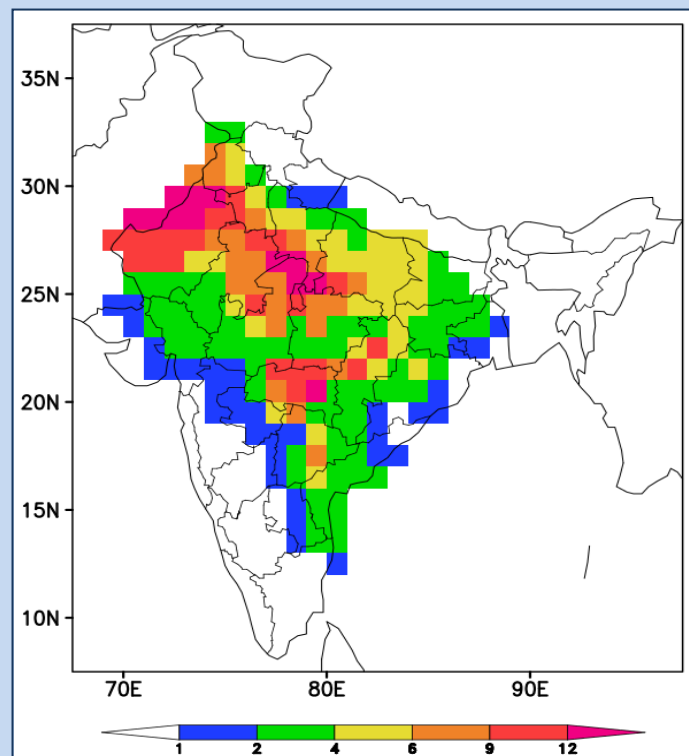


Diagnostics and Real-Time Extended Range Prediction of Heat Waves over India



Susmitha Joseph, R. Mandal, A. K. Sahai, R. Phani,
A. Dey and R. Chattopadhyay



Indian Institute of Tropical Meteorology (IITM)
Earth System Science Organization (ESSO)
Ministry of Earth Sciences (MoES)
PUNE, INDIA
<http://www.tropmet.res.in/>

ISSN 0252-1075
Contribution from IITM
Research Report No. RR-141
ESSO/IITM/SERP/SR/03(2018)/192

Diagnostics and Real-Time Extended Range Prediction of Heat Waves over India

**Susmitha Joseph, R. Mandal, A. K. Sahai, R. Phani,
A. Dey and R. Chattopadhyay**

***Corresponding Author Address:**

Dr. A.K. Sahai
Indian Institute of Tropical Meteorology,
Dr. Homi Bhabha Road, Pashan, Pune – 411 008, INDIA
E-mail: sahai@tropmet.res.in
Phone: +91-20-25904520



**Indian Institute of Tropical Meteorology (IITM)
Earth System Science Organization (ESSO)
Ministry of Earth Sciences (MoES)
PUNE, INDIA
<http://www.tropmet.res.in/>**

DOCUMENT CONTROL SHEET

Earth System Science Organization (ESSO)
Ministry of Earth Sciences (MoES)
Indian Institute of Tropical Meteorology (IITM)

ESSO Document Number

ESSO/IITM/SERP/SR/03(2018)/192

Title of the Report

Diagnostics and Real-Time Extended Range Prediction of Heat Waves over India

Authors

Susmitha Joseph, R. Mandal, A. K. Sahai, R. Phani, A. Dey, and R. Chattopadhyay

Type of Document

Scientific Report (Research Report)

Number of pages and figures

38, 14

Number of references

41

Keywords

Heat wave, extended range prediction, Ensemble Prediction System

Security classification

Open

Distribution

Unrestricted

Date of Publication

March 2018

Abstract

This study proposes a criterion for the *real-time* extended range prediction of heat waves based on the grand ensemble prediction system indigenously developed by the extended range prediction group of Indian Institute of Tropical Meteorology (IITM). It is found that the developed criterion is functional in providing outlook on the impending extreme temperatures with sufficient lead time.

Summary

Most parts of India suffers from spells of hot weather termed as *heat waves* during April - June, with high frequency over north, northwest, central and the eastern coastal regions of India. Studies indicate that with increasing global warming/climate change, the frequency and intensity of heat waves will increase. Therefore, understanding and predicting the extreme temperatures leading to heatwaves, are of greatest importance. The present study proposes a criterion for the *real-time* extended range prediction of heat waves. The grand ensemble prediction system based on National Centers for Environmental Prediction (NCEP) Climate Forecast System version 2 (CFSv2) developed by the extended range prediction group of Indian Institute of Tropical Meteorology (IITM) is used here for generating the extended range forecast. From the examples of some recent heat wave episodes, it is shown that the developed criterion has potential in providing outlook on the forthcoming extreme temperatures with sufficient lead time.

Contents

1.	Introduction	1
2.	Model and Observational Datasets	3
3.	Definition of Heat wave	4
3.1	Criteria proposed to identify and predict HW days in the present study	6
4.	Results and Discussions	7
4.1	Heat Wave Prone region	7
4.2	Identification of HW events based on different HW prone regions	8
4.3	Extended Range Prediction of HW events	8
4.3.1	Skill of the EPS in predicting extreme temperatures	9
4.3.2	Verification of the extended range prediction of some recent HW events	10
5.	Conclusion	13
	Acknowledgements	14
	References	15
	Figure Captions	20
	Figures	21

1. Introduction

With the increasing anthropogenic activities, the global temperature has shown an increasing trend in the present century (Parry et al., 2007; Hartmann et al., 2013). The increasing temperatures create discomfort and at times, the hot weather spells, which are otherwise known as *heatwaves* (hereafter termed as HW), can be deadly by claiming heavy toll of human lives as well as livestock (De and Mukhopdhyay, 1998). They can also cause serious problems to water supply, cause moisture reduction (stress is for crops) in the soil, influence the growth of crops, thereby adversely affecting agricultural production to a large extent (Chaudhuri et al., 2000; Attri and Rathore, 2003; Dash and Mamgain, 2011). The HW spells can lead to: increased energy demand, stress on energy supply infrastructure; increased demand for water; stress on infrastructures such as buildings, roads, rail etc.; shifts in tourism preferences due to higher temperatures; and increased risks for sporting and outdoor recreation activities.

Most parts of India suffer from spells of hot weather during April - June (AMJ), with high frequency over north, northwest, central and the eastern coastal regions of India. Generally, HWs develop in the northwestern parts of the country and progress towards neighbouring sub-divisions, especially over central and east India. On some occasions, they develop *in-situ* (Ray et al. 2013). HW can be driven by: (i) synoptic systems such as anticyclones, (ii) soil moisture and land surface interactions, and (iii) climate variability phenomena (Perkins, 2015 and references therein). The HWs over India have been linked with the climate modes such as El Niño-Southern oscillation or ENSO (De and Mukhopadhyay, 1998). Some studies also link them to the variations in the sea surface temperatures and re-curving tropical cyclones in the Bay of Bengal (Jenamani, 2012). The re-curving tropical cyclones before the onset of the HW could change the direction of the winds and cut-off moisture to the inland regions leading to HW (Jenamani, 2012; Ratnam et

al., 2016). [Ratnam et al. \(2016\)](#) indicated that the processes that maintain HWs over northwest-central and coastal eastern India could be different. They link the HWs of northwest-central India to anomalous blocking over North Atlantic and that over east coast to the anomalous cooling over central and east equatorial Pacific. [Rohini et al. \(2016\)](#) demonstrated that anomalous persistent high with anti-cyclonic flow, supplemented with clear skies and depleted soil moisture are primarily responsible for the occurrence of HW over India. They also showed that the variability of HW over India is influenced by both the tropical Indian Ocean and central Pacific SST anomalies.

Since HWs arise from extreme high temperatures, the increasing global warming can also lead to their increase. [Perkins et al. \(2012\)](#) noted an increasing observed global trend in the frequency, intensity and duration of warm spells and HW during 1950-2011. Based on the analysis of daily maximum and minimum temperature data of 121 stations well distributed over India during 1970–2005, [Kothawale et al. \(2010\)](#) showed that the frequency of occurrence of hot days and hot nights showed widespread increasing trend, while that of cold days and cold nights has shown widespread decreasing trend. [Rao et al. \(2005\)](#) indicated that southern peninsular India is showing more increasing trend in the day/night temperatures, compared to the northern India. Studies indicate that with rising global warming/climate change, the frequency and intensity of HW will increase ([Mearns et al. 1984](#); [Srivastava et al. 2001](#); [Manton, 2010](#); [Ray et al. 2013](#); [Murari et al., 2015](#); [Perkins, 2015](#); [Argüeso et al., 2016](#), [Ganguly et al., 2009](#) among others) and the mortality and morbidity rates due to HW are strongly linked to their duration and intensity ([Coumou et al. 2013](#)). [Russo and Sterl \(2011\)](#), based on the projections from a climate model, suggested significant increase in temperature extremes like warm days over the Indian region during the period 2001–2100. [Murari et al. \(2015\)](#), based on multiple climate models and scenarios for CMIP5 data, have shown that HWs are projected to be more intense, have longer

durations and occur at a higher frequency and earlier in the year. They also suggested that Southern India, currently not influenced by HW, is expected to be severely affected by the end of the twenty-first century. Although they expected this to occur towards the end of 21st century, the summer season of 2016, one of the warmest years of the century, witnessed the incidence of HW events in Kerala (situated at the southern tip of India) for the first time in its history, which is alarming. All these studies affirm the necessity of developing a strategy for forewarning and mitigation efforts to minimize adverse effects of HW over the country.

Although there are numerous studies on the mechanisms and projections of HW, very few studies have focused on their prediction (e.g. [Lee et al., 2016](#), [Pattnaik et al., 2016](#)). The efforts to predict HW in *real-time* using a dynamical frame work on extended range (ie., at least 10-15 days in advance) is still emergent. In the present study, a criteria has been developed that can be used not only to identify the HW episodes from observational datasets, but also to predict them on extended range time scale in *real-time*. The skill of an ensemble prediction system (EPS) in predicting the HW events will also be evaluated. It is expected that with improved extended range forecasts on impending HW, the loss of life and property can be reduced to a greater extend.

2. Model and Observational Datasets

The study makes use of the EPS indigenously developed at Indian Institute of Tropical Meteorology (IITM), enrooted on the Climate Forecast System version 2 (CFSv2) coupled model adopted from National Centre for Environmental Prediction (NCEP), USA, under the National Monsoon Mission (<http://www.tropmet.res.in/monsoon/>) project of Ministry of Earth Sciences, Government of India. The EPS consists of a suite of variants of the same model at different resolutions, such as: (i) CFSv2 at T382 (≈ 38 km) (ii) CFSv2 at T126 (≈ 100 km) (iii) GFSbc (the stand-alone atmospheric component - GFSv2, forced with bias corrected SST from CFSv2) at T382 and (iv) GFSbc at T126, all having 11 ensemble

members each (thus a total of 44 members) and also by using the atmospheric and oceanic initial conditions (ICs) available from NCEP once in every 5 days with forecast for 4 pentads. The details about the EPS and its skill analysis can be found in [Abhilash et al. \(2014a,b, 2015\)](#), [Sahai et al., \(2013, 2015\)](#) and [Borah et al. \(2013\)](#). The model runs are available for the period 2001-2016, with hindcast runs during 2001-2010.

For verification purposes, we use the maximum and minimum temperature datasets from IMD at $1^{\circ}\times 1^{\circ}$ resolution ([Srivastava et al. 2009](#)) that cover Indian land points only, for the period 1981-2016.

3. Definition of Heat wave

Although HWs represent periods of hotter than normal weather over a region, there is no universal definition for it. Most of the definitions are based on the persistence of maximum, minimum or mean surface air temperature above a threshold value that is based on the upper tail of the temperature distribution over a region ([Perkins, 2015](#)). Some of the definitions may even consider surface humidity levels as humidity can worsen a HW effect. According to [Vaidyanathan et al. \(2016\)](#), a HW definition has four core variables - the heat metric (viz., maximum/minimum/mean temperature, diurnal temperature difference etc.), duration, threshold type and threshold intensity.

[Della-Martha et al. \(2007\)](#) defined HW as the number of consecutive 3-day periods in summer that exceed the long-term daily 80th percentile of daily maximum temperature, while [Srivastava et al. \(2009\)](#) defined the event if the maximum temperature at a grid point is 3°C or more than the normal temperature, consecutively for 3 days or more. [Mishra et al. \(2015\)](#) considered HW as periods during which the daily maximum temperature stayed above the empirical 99th-percentile consecutively for six or more days. [Ganguly et al. \(2009\)](#) defined HW as the mean annual consecutive 3-day warmest night-time minima event. Apart from temperature, large scale circulation has also been used to define HW, as

in Lee et al. (2016) where a HW index over Korea is given as difference in the 200 hPa vorticity between the average over 25°–30°N, 110°–130°E and the average over 35°–45°N, 120°–140°E. Australian Bureau of Meteorology defines the HW using Excess Heat Factor (EHF) (Nairn et al., 2013; Nairn and Fawcett, 2013, 2015; Perkins and Alexander, 2013), which in turn depends on Excess Heat and Heat Stress. Both maximum and minimum temperatures are used in this assessment. Daily mean temperature averaged over a three day period against its climatological value is used to characterize excess heat, while maximum and subsequent minimum averaged over a three-day period and the previous 30 days characterizes heat stress.

The definition specified by India Meteorological Department (IMD) for station data has been widely used in many studies (De and Mukhopadhyay, 1998; Chaudhury et al., 2000; Pai et al., 2004, 2013, 2017; Ray et al., 2013; Ratnam et al., 2016, among others). The criteria set by IMD is as follows:

When maximum temperature of a station reaches $\geq 40^{\circ}\text{C}$ for plains and $\geq 30^{\circ}\text{C}$ for hilly regions,

(a) Based on departure from normal: HW: maximum temperature departure from normal is 4.5°C to 6.4°C

Severe HW (SHW): maximum temperature departure from normal is $\geq 6.5^{\circ}\text{C}$

(b) Based on actual maximum temperature:

HW: actual maximum temperature is $\geq 6.5^{\circ}\text{C}$

SHW: actual maximum temperature is $\geq 47^{\circ}\text{C}$

(c) Criteria for coastal stations:

HW: When maximum temperature departure $\geq 4.5^{\circ}\text{C}$ and actual maximum temperature $\geq 37^{\circ}\text{C}$

3.1 Criteria proposed to identify and predict HW days in the present study

Since our criteria should match with that of IMD, which is based on station data, the following criteria is proposed in the present study for the real time monitoring and prediction of HW and SHW based on gridded data.

- A. If maximum temperature is $\geq 39^{\circ}\text{C}$ and minimum temperature $\geq 90^{\text{th}}$ percentile of the observed minimum temperature for that day
- B. If maximum temperature $\geq 95^{\text{th}}$ percentile of the observed maximum temperature for that day, and actual maximum temperature is $\geq 39^{\circ}\text{C}$, and maximum temperature departure from normal is $\geq 3.5^{\circ}\text{C}$
OR maximum temperature is $\geq 44^{\circ}\text{C}$
- C. If maximum temperature $\geq 99^{\text{th}}$ percentile of the observed maximum temperature for that day, and actual maximum temperature is $\geq 39^{\circ}\text{C}$, and maximum temperature departure from normal is $\geq 5.5^{\circ}\text{C}$
OR maximum temperature is $\geq 46^{\circ}\text{C}$

If a particular day satisfies A, it is called hot day (hereafter referred as HOT); if it satisfies B, it is HW condition and; if satisfying C, it is a SHW condition. The definitions are such a way that most of the HOT conditions are inclusive of HW, and HW includes SHW.

Since the CFSv2 model is known to have a temperature bias ([Abhilash et al., 2014b](#); [Sahai et al., 2013](#)), the temperature from the model has been bias corrected with respect to the observed climatology during the hindcast period. Daily observed percentiles of maximum/minimum temperature have been calculated for the period 1981-2010 and have been used to calculate the extreme heat conditions on the model forecasted bias corrected data.

The probability of extreme heat conditions, viz., HOT, HW and SHW have been calculated based on the percentage (%) of ensemble members satisfying the conditions mentioned in A, B and C.

4. Results and Discussions

4.1 Heat Wave Prone region

Based on the criteria proposed in the section 3.1, we have calculated the HW days during 1981-2015 for the observational maximum/minimum temperature data. The total number of HW days per year is shown in **Figure 1**. It is clear from the figure that the northwest India comprising Punjab, Rajasthan, Haryana and Delhi; central India including Madhya Pradesh, Chattisgarh, northeast Maharashtra (*called* Vidarbha); and southeastern state of Telengana experiences more than 6 HW days /year. Other regions that are susceptible to HW conditions (having an average of > 2 HW days/year) are: Andhra Pradesh, Orissa, Jharkhand, Bihar, Uttar Pradesh, northwest West Bengal and Gujarat. Based on the observed patterns and statistical analyses of the maximum temperature variability, [Ratnam et al. \(2016\)](#) identified two regions that are vulnerable to HW, i.e., north-central India and coastal eastern India, and showed that both of them are maintained by different processes. Here, depending on the average number of HW days, regions with >2 HW days/year are considered as the HW prone regions. Among those, the region above 22°N is termed as northwest (NW) region, and that below 22°N as southeast (SE) region (**Figure 2**). At times, some HW events originate over NW region and move towards SE region with time, such as the one happened during the second half of May 2015 ([Pattanaik et al. 2016](#)). Therefore, we have identified the northwest-southeast region (NWSE) which comprises both the NW and SE regions, also to account for such events.

4.2 Identification of HW events based on different HW prone regions

Ratnam et al. (2016) identified HW events when the normalized area averaged Tmax anomalies are greater than one standard deviation for 6 days or more consecutively over the two regions selected by them. Here, we identify the HW events over NW/SE regions when the actual Tmax values area averaged over the region exceed 41°C for a minimum of consecutive 5 days. In addition, the spells over NWSE region are identified from the spells over NW and SE regions, that overlap with each other. The HW spells thus identified over NW, SE and NWSE regions, during 1981-2016 are given in **Table-1**.

Figure 3 shows the actual and anomaly values of tmax composited for the HW spells identified for NW, SE and NWSE regions. The *top panels* show the actual values, while *bottom panels* depict the anomalous values. It is found that during HW spells over NW region, the maximum heating is observed over NW and central parts of the country (*top and bottom left panels*), while during that over SE region, the heating is maximum over southeastern coastal parts (*top and bottom middle panels*). In the case of NWSE region, the warming is noticed almost all over the country, except parts of the peninsula and northeastern states. This clearly indicates that these three types of HWs are distinct in the spatial distribution of temperatures. However, as this study highlights on the development and evaluation of a HW criterion for *real-time* prediction, the identification of the causative mechanisms behind each of the HW types is beyond the scope of the present study.

4.3 Extended Range Prediction of HW events

Before analyzing the skill of the EPS in predicting HW events, it is important to document it's general skill in predicting extreme heat conditions. This is evaluated in the next section.

4.3.1 Skill of the EPS in predicting extreme temperatures

Since HW episodes arise from abnormal extreme temperatures, the skill of the EPS in terms of pentad-wise (Pentad 1 to Pentad 4) anomaly correlation coefficient (ACC) of t_{max} and t_{min} for all pentads during AMJ for the hindcast period is shown in **Figure 4**. Correlations, significant at 99.9% significance level, are only shaded in the figure. It is clear from the figure that the ACCs for t_{max} and t_{min} are significant up to P4 lead over most parts of the country, with remarkable values over the HW regions (mentioned in **Figures 2** and **3**) during all 4 pentad leads.

Another skill score that can exemplify usefulness of the EPS in extreme event prediction is the Symmetric Extremal Dependence Index (SEDI; (Ferro and Stephenson 2011)) which is widely used for the verification of deterministic forecasts of rare events. It is defined as:

$$SEDI = \frac{\log F - \log H - \log(1 - F) + \log(1 - H)}{\log F + \log H + \log(1 - F) + \log(1 - H)}$$
$$= \frac{\log(F(1 - H)/H(1 - F))}{\log(F(1 - F)H(1 - H))}$$

where, $H = \frac{a}{a + c}$ is the hit rate and $F = \frac{b}{b + d}$ is the false-alarm rate. a , b , c , and d are the number of hits, the number of false-alarms, the number of misses and the number of correct rejections respectively – the elements of the 2×2 contingency table).

The SEDI values above zero imply that the forecast system is better than random, values below zero allude a forecast system which is worse.

Figure 5 shows the pentad-wise (P1 to P4 lead) SEDI values for 70, 50 and 30 percentage probabilities of HOT category. It is found that the EPS is skillful in predicting the HOT conditions up to 4th pentad lead even with 70% probability. It is interesting to note that the maximum SEDI values are seen over HW prone regions (as shown in Figures 1 and 2). **Figures 6** and **7** show the SEDI values of HW and SHW categories respectively. The SEDI values are skillful with 50% and 30% probabilities over the HW prone regions (*second and third columns of Figure 6*). However, the SEDI values decrease with 70% probability of HW category, especially at the P4 lead. In case of SHW category, the SEDI values are skillful only over northwest, and parts of central and southeast India (*third column of Figure 7*).

Thus, based on the values of ACC and SEDI, it is recognized that the EPS is beneficial for HW prediction.

4.3.2 Verification of the extended range prediction of some recent HW events

In the previous section, the general prediction skill of the EPS in forecasting extreme temperatures has been documented. Now, the proficiency of the EPS in predicting the some of the recent HW events will be examined in this section. *(i) Event 1: 15-21 May 2008*

During this period, the SE parts of the country experienced HW conditions. The probability of occurrence of the event and the tmax anomalies during the period is given in **Figure 8**. The *top panel* shows the observed probability (in %; *top left panel*) and observed tmax anomalies (in °C; *top right panel*) of the event during the period and the subsequent *left (right)* panels show the predicted HW probabilities (tmax anomalies) from nearest (IC: 11 May or 0511) to farthest (IC: 26 April or 0426) ICs. It is found that though the MME could predict the event from almost all the four ICs to some extent, the probabilities are very less, compared to the observed values. It is also noted that the MME gave some false signals

over east coast and parts of north and central India. Even though the tmax anomalies are weak, the MME got successful in providing an indication of the impending event.

(ii) Event 2: 12 May - 03 June 2010

This was one of the severe HWs that embraced the northwestern and central parts of the country resulting in high rate of mortality. The observed and predicted probabilities for the event is shown in the *left column* of **Figure 9**. It is found that the spell was indeed predicted by the MME from almost all leads, with probabilities decreasing with increasing lead. It is also noticed that the MME falsely gave indications of HW conditions over southeastern parts of India. The tmax anomalies shown in the *right column* of the figure indicates that the increased positive anomalies over the HW affected regions were well predicted from the nearest IC (11 May). It is interesting to note that the tmax anomalies could give an indication of the positive sign of tmax anomalies over Gujarat region from the 26 April IC.

(iii) Event 3: 02-11 June 2014

This HW spell during early June 2014 could be related to the weak northward progression of southwest monsoon, and affected the northwest parts of the country. *Left column* of **Figure 10** depicts the observed and predicted probabilities of the event. This is one of the *best-predicted* HW spell, as it was predicted very well from the nearest two ICs (31 May and 26 May), and to some extent from 21 May and 16 May ICs. The tmax anomalies also corroborate the observed and predicted probabilities (*right column* of **Figure 10**).

(iv) Event 4: 18-31 May 2015

The May 2015 event was one of the deadliest HWs that affected the eastern coastal states, central and northwestern parts of the country and claimed casualties of more than 2500 people ([Pattanaik et al. 2016](#)). It is noticed that almost all nearest to farthest ICs (16

May, 11 May, 06 May, 01 May) could give an indication of the imminent HW event (*left panels* of **Figure 11**). The positive tmax anomalies over eastern states during the period were very well predicted by 16 May, 06 May and 01 May ICs (*right panels* of **Figure 11**).

(v) Event 5: 19 April- 03 May 2016

The year 2016 witnessed three HW events during the study period (refer **Table 1**). The first spell in this series is the one happened towards the second half of April 2016. The eastern parts of the country experienced extreme temperatures during this period. **Figure 12** illustrates the observed as well as predicted HW probabilities (*left panels*) and tmax anomalies (*right panels*) for the HW period. The event was predicted to some extent from 16 April and 11 April ICs. The MME failed to predict the event from 06 April IC.

(vi) Event 6: 12-28 May 2016

The second spell in 2016 happened during 12-28 May, and the regions affected by the HW were northwest and central India and some southeastern states of the country. The HW conditions over northwest and central parts were pretty well predicted from the nearest IC - 11 May (**Figure 13**). The predictions were realistic from 01 May IC. The HW conditions over central India were predicted with reasonable probability from the ICs - 06 May and 26 April (*left panels* of the figure).

(vii) Event 7: 03-07 June 2016

The last HW event happened in 2016 was in the first week of June and the northwest India got affected by it. An outlook on the event was obtained from the nearest (31 May) and farthest (16 May) ICs (**Figure 14**). The MME failed to predict the event from 21 May IC. The predictions from 26 May IC falsely predicted HW conditions over central India.

5. Conclusions

This study proposes a criterion for the *real-time* monitoring and extended range prediction of heat waves over India during AMJ using the grand ensemble prediction system, based on NCEP-CFSv2, developed at IITM. Since the CFSv2 model has a temperature bias, the temperature from the model has been bias corrected w.r.t the observed climatology. The proposed criterion is similar to the one used by IMD, but with slight modifications to suit the gridded data. Three categories, viz., HOT, HW and SHW have been defined using the thresholds of actual actual tmax values, departures from normal and the percentiles. Depending on the average number of HW days, regions with >2 HW days/year are considered as the HW prone regions. Among those, the region above 22°N is termed as northwest (NW) region, and that below 22°N as southeast (SE) region. The northwest-southeast region (NWSE) which comprises both the NW and SE regions, is also identified. It is found that during HW spells over NW region, the maximum heating effect is observed over NW and central parts of India, while during that over SE region, the heating is maximum over southeastern coastal parts.

Anomaly Correlation Coefficient (ACC) of tmax and tmin for all 4 pentads during AMJ for the hindcast period are significant over most parts of the country, with remarkable values over the HW-prone areas. The SEDI score values are calculated for 70, 50 and 30 percentage probabilities of HOT, HW and SHW categories. It is found that the EPS is skillful up to 4th pentad lead in predicting the HOT conditions, even with 70% probability. It is interesting that the SEDI values for HW and SHW categories are skillful over the HW prone regions, i.e., the northwest India and parts of central and southeast India. Therefore, based on the values of ACC and SEDI, it is identified that the EPS is beneficial for HW prediction.

The robustness of the proposed criteria has been verified for some recent HW events. It is noticed that though the MME could predict those events at sufficient lead time, the probabilities are very less for some of the events, compared to the observed values. It is also noted that the MME gave some false signals over east coast and parts of north and central India for some of the cases. Overall, it is shown that the developed criterion has potential in providing an outlook on the forthcoming HW spells with sufficient lead time.

Acknowledgement: IITM is fully supported by the Ministry of Earth Sciences, Govt. of India, New Delhi. The model runs are carried out on the AADITYA High Performance Computing facility installed at IITM, Pune. We thank NCEP for analysis datasets and technical support on CFSv2 model. We are also thankful to IMD for providing daily gridded temperature data.

Table 1: The heat wave spells identified for different heat wave prone regions. The duration of each spell is given in brackets.

NW	SE	NWSE
1989: 17-24 May (8)	1983: 29 May- 05 Jun (8)	1984: 17-29 May (13)
1992: 03-08 Jun (6)	1994: 07-14 May (8)	1988: 07-14 May (8)
1993: 06-12 Jun (7)	1996: 10-17 May (8)	1988: 22 May - 01 Jun (11)
1994: 27 May -09Jun (14)	1997: 19-25 May (7)	1998: 18 May - 08 Jun (22)
1995: 26 May - 10 Jun (16)	1997: 26 May - 02 Jun (8)	2003: 17May - 12 Jun (27)
1999: 24 Apr - 07 May (14)	2001: 09-14 May (6)	2005: 11-20 Jun (10)
2005: 01-06 Jun (6)	2002: 09-15 May (7)	2010: 12 May - 03 Jun (23)
2010: 14-19 Apr (6)	2005: 14-19 May (6)	2012: 17 May - 09 Jun (24)
2014: 02-11 Jun (10)	2007: 15-22 May (8)	2013: 17-26 May (10)
2016: 03-07 Jun (5)	2008: 15-21 May (7)	2015: 18-31 May (14)
		2016: 19 Apr -03 May (15)
		2016: 12-28 May (17)

References

Abhilash, S., Sahai, A.K., Pattnaik, S., Goswami, B. N., Kumar, A., 2014a, Extended Range Prediction of Active-Break Spells of Indian Summer Monsoon Rainfall using an Ensemble Prediction System in NCEP Climate Forecast System, *Int. J. Climatol.*, **34**, January 2014, DOI:10.1002/joc.3668, 98-113.

Abhilash, S., Sahai, A.K., Borah, N., Chattopadhyay, R., Joseph, S., Sharmila, S., De, S., and Goswami, B. N., 2014, Does bias correction in the forecasted SST improves the extended range prediction skill of active-break spells of Indian summer monsoon rainfall?, *Atmos. Sci. Lett.*, **15**, June 2014, DOI:10.1002/asl2.477, 114–119.

Abhilash. S, Sahai, A.K., Borah, N., Joseph, S., Chattopadhyay, R., Sharmila, S., Rajeevan, M., Mapes, B., and Kumar, A., 2015, Improved Spread-Error Relationship and Probabilistic Prediction from CFS based Grand Ensemble Prediction System, *J. Appl. Meteorol. Climatol.*, **Volume 54**, Issue 7 (July 2015) pp. 1569-1578, doi:10.1175/JAMC-D-14-0200.1

Argüeso, D., Di Luca, A., Perkins-Kirkpatrick, S., and Evans, J. P., (2016), Seasonal mean temperature changes control future heat waves, *Geophys. Res. Lett.*, **43**, 7653–7660, doi:10.1002/2016GL069408.

Attri, S. D., and Rathore, L. S., 2003, Simulation of impact of projected climate change on wheat in India, *Int. J. Climatol.*, **23**, 693–705, doi:10.1002/joc.896.

Borah, N., Abhilash, S., Joseph, S., Chattopadhyay, R., S., Sharmila, and Sahai, A.K., 2013, Development of Extended Range Prediction System Using CFSv2 and Its verification, *IITM Res. Rep.*, **RR-130**, ISSN 0252-1075, pp 1-62.

Chaudhury, S.K., Gore, J.M., and Sinha Ray, K.C., 2000, Impact of heat waves over India, *Curr Sci.*, **79**:153–155

Coumou, D., Robinson, A., and Rahmstorf, S., 2013, Global increase in record-breaking monthly-mean temperatures, *Climatic Change*, **118**, 771-782. <https://doi.org/10.1007/s10584-012-0668-1>.

Dash, S.K., and Mangain, A., 2011, Changes in the frequency of different categories of temperature extremes in India, *J. Appl. Meteorol. Climatol*, **50**, 1842–1858.

De, U.S. and Mukhopadhyay, R.K., 1998, Severe heat wave over Indian subcontinent in 1998 in a perspective of global Climate, *Current Science*, **75**, 12, 1308-1311.

Della-Marta, P.M., Luterbacher, J., Weissenfluh, H. von, Xoplaki, E., Brunet, M., and Wanner, H., 2007, Summer heat waves over western Europe 1880–2003, their relationship to large-scale forcings and predictability, *Clim Dyn*, **29**, 251–275, DOI 10.1007/s00382-007-0233-1.

Ferro, C.A.T., and Stephenson, D.B., 2011, Extremal dependence indices: improved verification measures for deterministic forecasts of rare binary events, *Weather Forecast*, **26**, 699–713.

Ganguly, A.R., Steinhäuser, K., Erickson, D.J., Branstetter, M., Parish, E.S., Singh, N., Drake, J.B., and Buja, L., 2009, Higher trends but larger uncertainty and geographic variability in 21st century temperature and heat waves, *PNAS*, September 15, **vol. 106**, no. 37: 15555–15559, doi: 10.1073_pnas.0904495106

Hartmann, D.L., Klein Tank, A.M.G., Rusticucci, M., Alexander, L., Brönnimann, S., Charabi, Y., Dentener, F., Dlugokencky, E., Easterling, D., Kaplan, A., Soden, B., Thorne, P., Wild, M., and Zhai, P.M., 2013, Observations: Atmosphere and Surface Supplementary Material. In: *Climate Change 2013: The Physical Science Basis. Contribution of Working Group I to the Fifth Assessment Report of the Intergovernmental Panel on Climate Change* [Stocker, T.F., Qin, D., Plattner, G.K., Tignor, M., Allen, S.K., Boschung, J., Nauels, A., Xia, Y., Bex, V., and Midgley, P.M., (eds.)].

Parry, M.L., Canziani, O.F., Palutikof, J.P., Van der Linden, P.J., and Hanson, C.E., Eds., *IPCC, Climate Change 2007, Impacts, Adaptation and Vulnerability. Contribution of Working Group II to the Fourth Assessment Report of the Intergovernmental Panel on Climate Change*, (Cambridge University Press, 2007).

Jenamani, R.K., 2012, Analysis of Ocean-Atmospheric features associated with extreme temperature variations over east coast of India - A special emphasis to Orissa heat waves of 1998 and 2005. *Mausam*, **63**, 401–422.

Kothawale, D.R., Revadekar, Jayashree V. and K. Rupa Kumar, 2010, Recent trends in pre-monsoon daily temperature extremes over India, *Journal of Earth System Science*, **119(1)**, 51-65.

Lee, H.J., Lee, W.S., and Yoo, J. H., 2016, Assessment of medium-range ensemble forecasts of heat waves, *Atmos. Sci. Lett.*, **17**, 19–25. doi:10.1002/asl.593.

Manton, M.J., 2010, Trends in climate extremes affecting human settlements, *Curr Opin Environ Sustain*, **2**, 151–155.

Mearns, L.O., Katz, R.W., and Schneider, S. H., 1984, Extreme high-temperature events: Changes in their probabilities with changes in mean temperature, *J. Clim.*, **23**, 1601–1613.

Mishra, V., Ganguly, A.R., Nijssen, B., and Lettenmaie, D. P., 2015, Changes in observed climate extremes in global urban areas, *Environ. Res. Lett.*, **10**, 024005. <https://doi.org/10.1088/1748-9326/10/2/024005>.

Murari, K.K., Ghosh, S., Patwardhan, A., Daly, E., and Salvi, K., 2015, Intensification of future severe heat waves in India and their effect on heat stress and mortality, *Reg. Environ Change*, **15**, 569–579; doi: 10.1007/s10113-014-0660-6 (2015).

Nairn, J., and Fawcett, R., 2013, Defining heatwaves: Heatwave defined as a heat impact event servicing all community and business sectors in Australia, *CAWCR. Technical Report No 060*.

Nairn, J., and Fawcett, R., 2015, The Excess Heat Factor: A Metric for Heatwave Intensity and Its Use in Classifying Heatwave Severity, *Int. J. Environ. Res. Public Health*, **12**, 227–253; doi:10.3390/ijerph120100227

Pai, D.S., Thapliyal, V., and Kokate, P.D., 2004, Decadal variation in the heat and cold waves over India during 1971–2000, *Mausam*, **55**, 281–292.

Pai, D.S., Smitha, A., and Ramanathan, A. N., 2013, Long term climatology and trends of heat waves over India during the recent 50 years (1961–2010), *Mausam*, **64(4)**, 585–604 .

Pai, D.S., Srivasatava, A.K., and Smitha, A., 2017, Heat and Cold waves over India, chapter 4 in *Observed climate variability and change over the Indian region*, Rajeevan, M., and Nayak, S. (eds.), *Springer Geology*, DOI: 10.1007/978-981-10-2531-0_4

Pattanaik, D.R., Mohapatra, M., Srivastava, A.K., and Kumar, A, 2017, Heat wave over India during summer 2015: an assessment of real time extended range forecast, *Meteorol Atmos Phys*, 129: 375. <https://doi.org/10.1007/s00703-016-0469-6>.

Perkins, S.E., Alexander, L.V., and Nairn, J.R., 2012, Increasing frequency, intensity and duration of observed global heatwaves and warm spells, *Geophys. Res. Lett.* **39**, L20714, doi: 10.1029/2012GL051120.

Perkins, S.E., and Alexander, L.V., 2013, On the Measurement of Heat Waves, *J. Clim.*, **26**, 4500–4517, doi: 10.1175/JCLI-D-12-00383.1.

Perkins, S. E., 2015, A review on the scientific understanding of heatwaves—their measurement, driving mechanisms and changes at the global scale, *Atmos Res.*, 164–165, 242–267.

Rao, G.S.P., Murthy, M.K., and Joshi, U. R., 2005, Climate change over India as revealed by critical extreme temperature analysis; *Mausam*, 56 601–608

Ratnam, J.V., Behera, S. K., Ratna, S. B., Rajeevan, M., and Yamagata, T., 2016, Anatomy of Indian heatwaves, *Sci. Rep.*, **6**, 24395, doi: 10.1038/srep24395.

Ray, K., Chincholikar, J.R., and Mohanty, M., 2013, Analysis of extreme high temperature conditions over Gujarat, *Mausam*, **64**, 3: 467-474.

Rohini, P., Rajeevan, M., and Srivastava, A.K., 2016, On the variability and increasing trends of heat waves over India, *Sci. Rep.*, **6**, 26153.

Russo, S., and Sterl, A., 2011, Global changes in indices describing moderate temperature extremes from the daily output of a climate model, *Journal of Geophysical Research*, **VOL. 116**, D03104, doi:10.1029/2010JD014727.

Sahai, A.K., Sharmila, S., Abhilash, S., Chattopadhyay, R., Borah, N., Krishna, R.P.M., Joseph, S., M., Roxy, De, S., Pattnaik, S., and Pillai, P.A., 2013, Simulation and extended range prediction of monsoon intraseasonal oscillations in NCEP CFS/GFS version 2 framework, *Curr. Sci.*, **104**, 1394–1408.

Sahai, A.K., Abhilash, S., Chattopadhyay, R., Borah, N., Joseph, S., Sharmila, S., and Rajeevan, M., 2015, High Resolution operational Monsoon Forecasts: An Objective Assessment, *Climate Dynamics*, **44**, 3129–3140, DOI 10.1007/s00382-014-2210-9

Srivastava, A.K., Sinha Ray, K.C., and Yadav, R.V., 2001, “Is summer becoming more uncomfortable over major cities of India?”, *Current Science*, **Vol. 81**, No. 4, pp. 343-344.

Srivastava, A.K., Rajeevan, M., and Kshirsagar, S.R., 2009, Development of a high resolution daily gridded temperature data set (1969–2005) for the Indian region, *Atmos. Sci. Lett.*, **10**, 249–254, doi:10.1002/asl.232.

Vaidyanathan, A., Kegler scott, R., Saha, S.S., and Mulholland, J.A., 2016, A Statistical Framework to Evaluate Extreme Weather Definitions from A Health Perspective: A Demonstration Based on Extreme Heat Events, *Bulletin of the American Meteorological Society*, **97(10)**, 1817-1830, doi:10.1175/BAMS-D-15-00181.1.

List of Figures

- Figure 1:** The total number of HW days per year, calculated during 1981-2015 for the observed maximum/minimum temperature data.
- Figure 2:** North-West (NW) region (red-coloured) above 22°N and South-East (SE) region (blue-coloured) below 22°N. The region comprising both NW and SE is defined as NWSE region.
- Figure 3:** Actual and anomaly values of Tmax composited for the HW spells identified for NW, SE and NWSE regions. The top panels show the actual values, while bottom panels depict the anomalous values.
- Figure 4:** Pentad-wise (Pentad 1 to Pentad 4) anomaly correlation coefficient (ACC) of tmax and tmin during April-June (AMJ) for all the pentads during hindcast period (2001-10). Correlations are significant at 99.9% significance level.
- Figure 5:** Pentad-wise (P1 to P4 lead) SEDI values for 70, 50 and 30 percentage probabilities of HOT category.
- Figure 6:** Same as Figure 5, but for HW category.
- Figure 7:** Same as Figure 5, but for SHW category.
- Figure 8:** The probability of occurrence of HW event (left column) and the tmax anomalies (right column) during the period 15-21 May 2008 for observation (top panels) and model (subsequent panels).
- Figure 9:** Same as Figure 8, but for the HW during 12 May - 3 June 2010.
- Figure 10:** Same as Figure 8, but for the HW during 2-11 June 2014.
- Figure 11:** Same as Figure 8, but for the HW during 18-31 May 2015.
- Figure 12:** Same as Figure 8, but for the HW during 19 April - 3 May 2016.
- Figure 13:** Same as Figure 8, but for the HW during 12-28 May 2016.
- Figure 14:** Same as Figure 8, but for the HW during 3-7 June 2016.

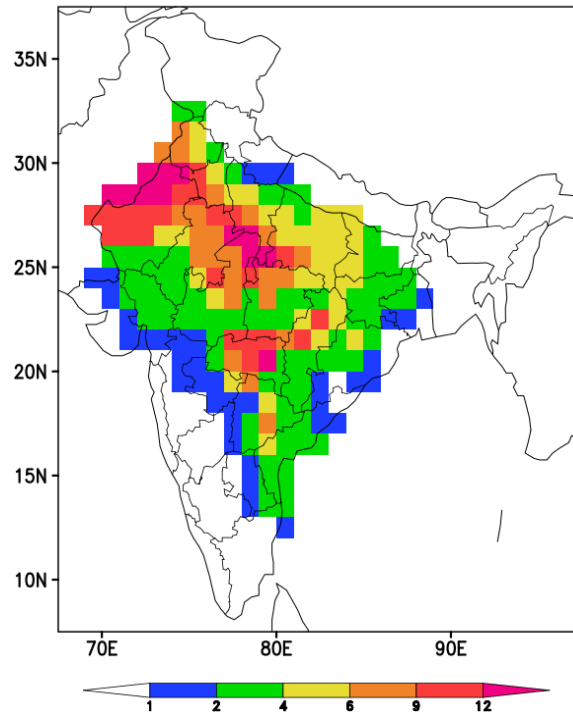


Figure1: The total number of HW days per year, calculated during 1981-2015 for the observed maximum/minimum temperature data.

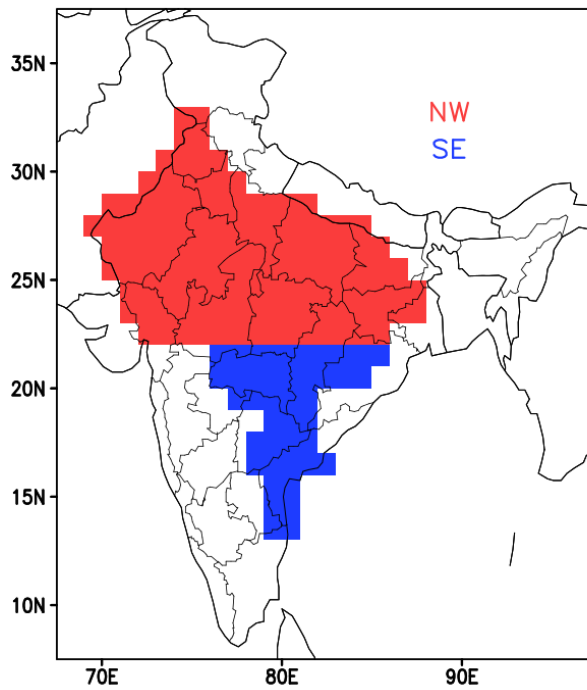


Figure 2: North-West (NW) region (red-coloured) above 22°N and South-East (SE) region (blue-coloured) below 22°N. The region comprising both NW and SE is defined as NWSE region.

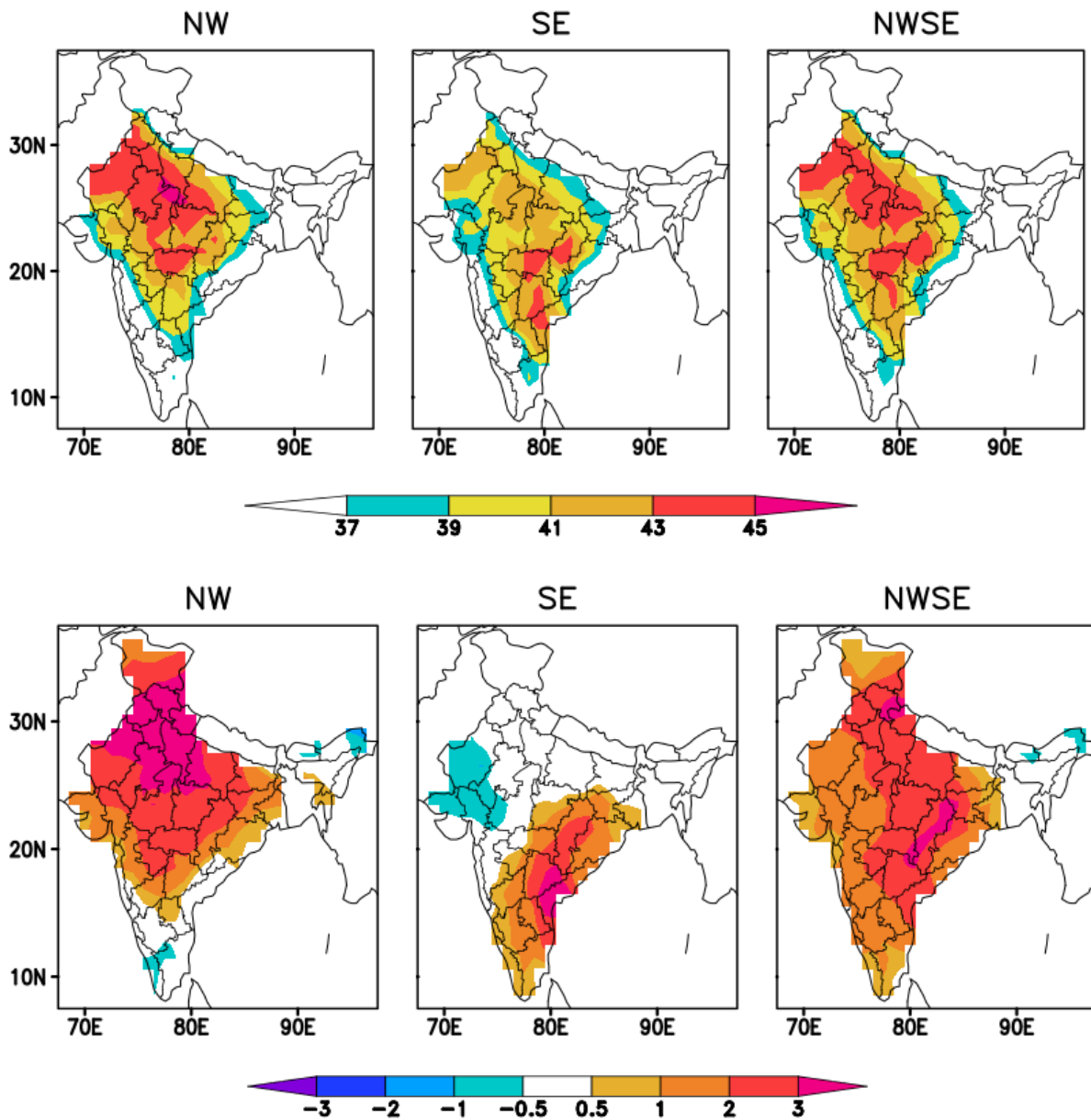


Figure 3: Actual and anomaly values of Tmax composited for the HW spells identified for NW, SE and NWSE regions. The top panels show the actual values, while bottom panels depict the anomalous values.

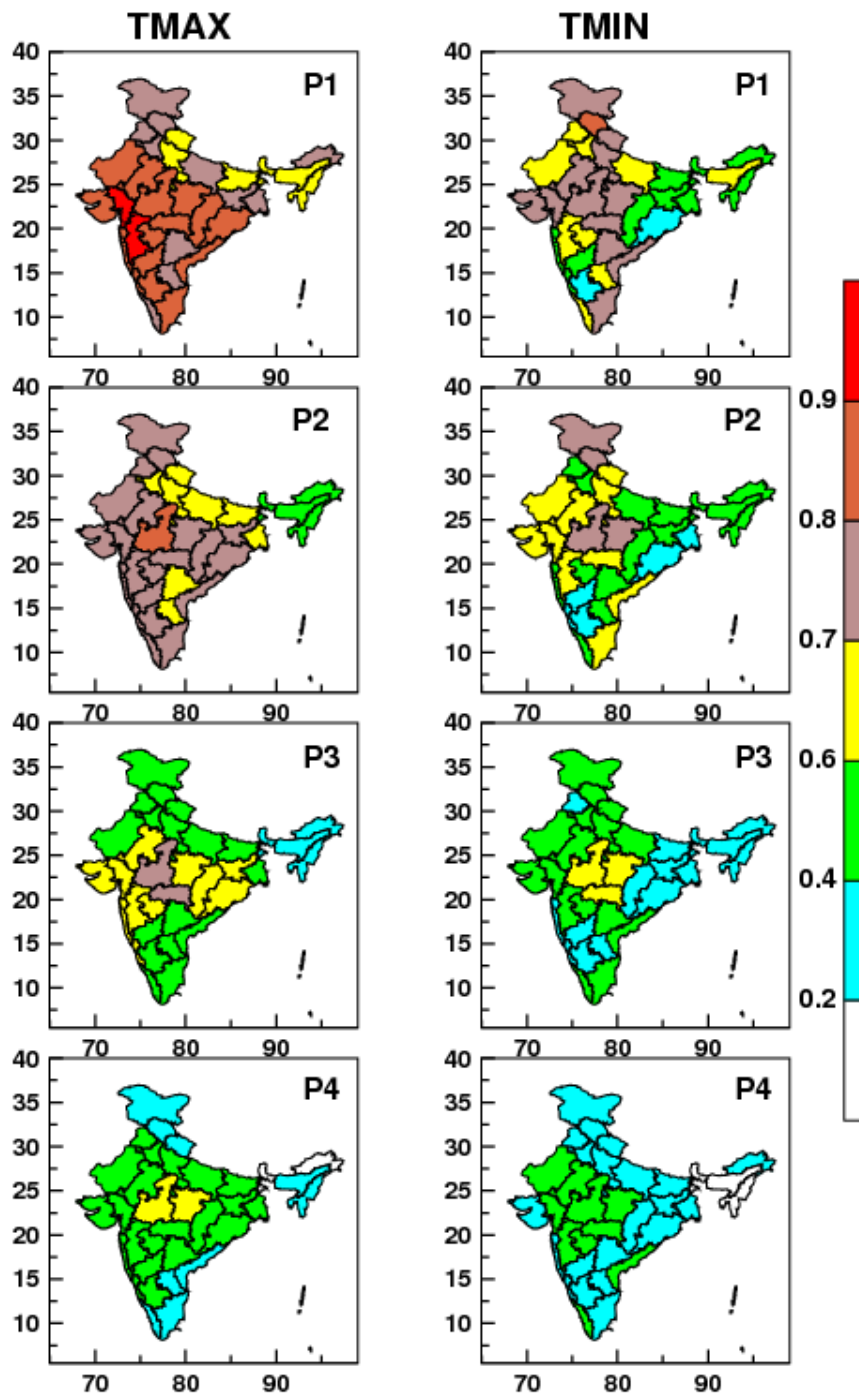


Figure 4: Pentad-wise (Pentad 1 to Pentad 4) anomaly correlation coefficient (ACC) of tmax and tmin during April-June (AMJ) for all the pentads during hindcast period (2001-10). Correlations are significant at 99.9% significance level.

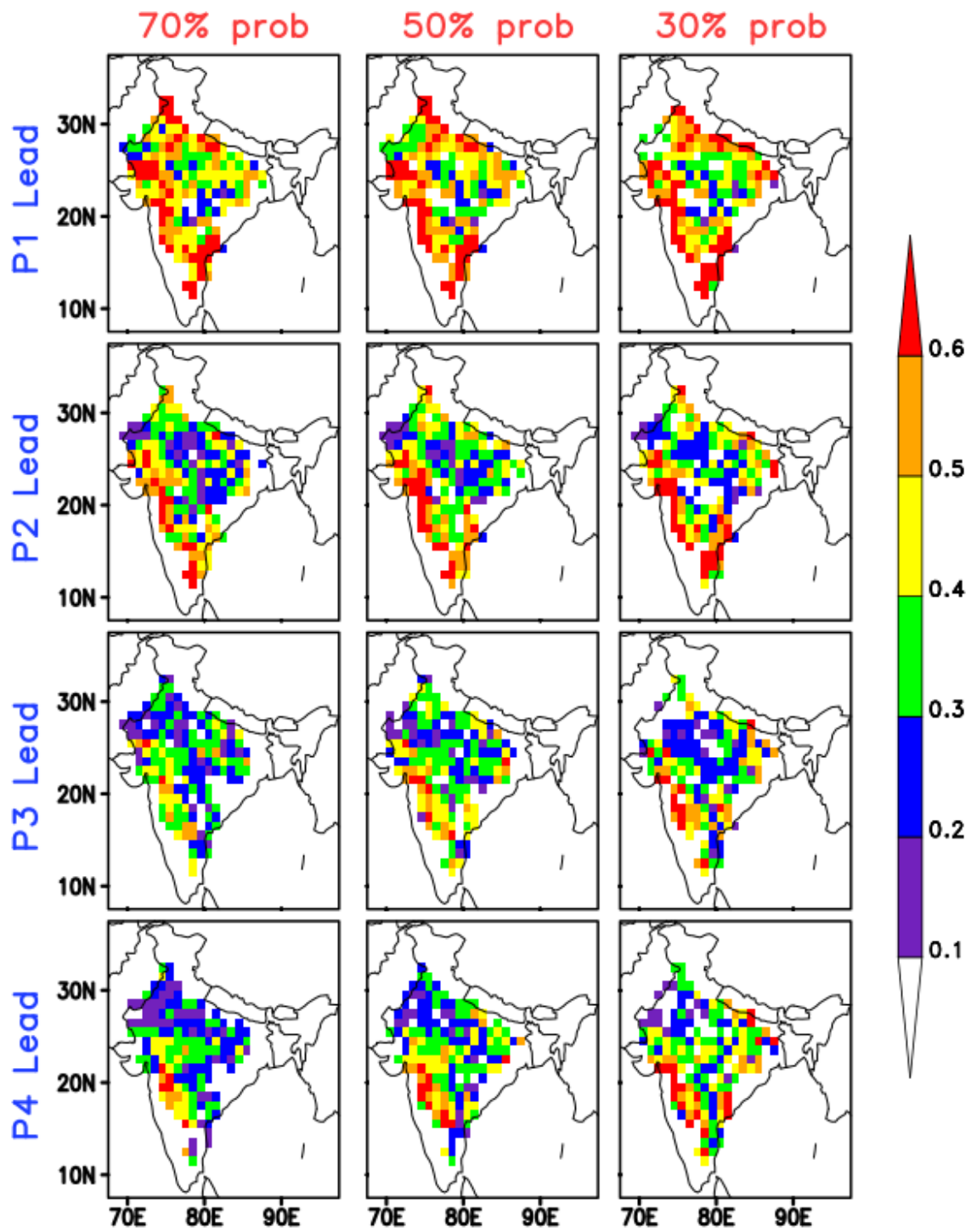


Figure 5: Pentad-wise (P1 to P4 lead) SEDI values for 70, 50 and 30 percentage probabilities of HOT category.

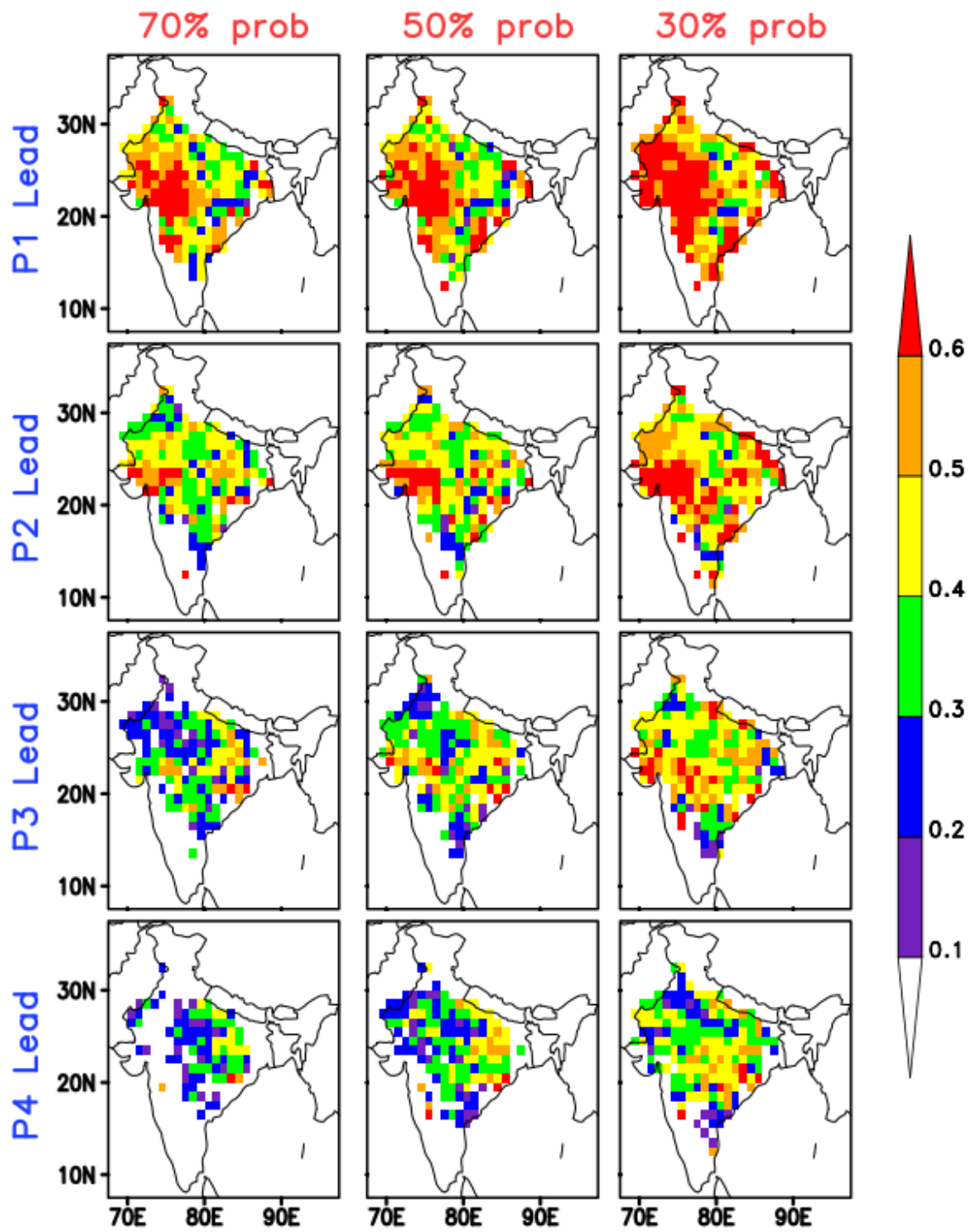


Figure 6: Same as Figure 5, but for HW category.

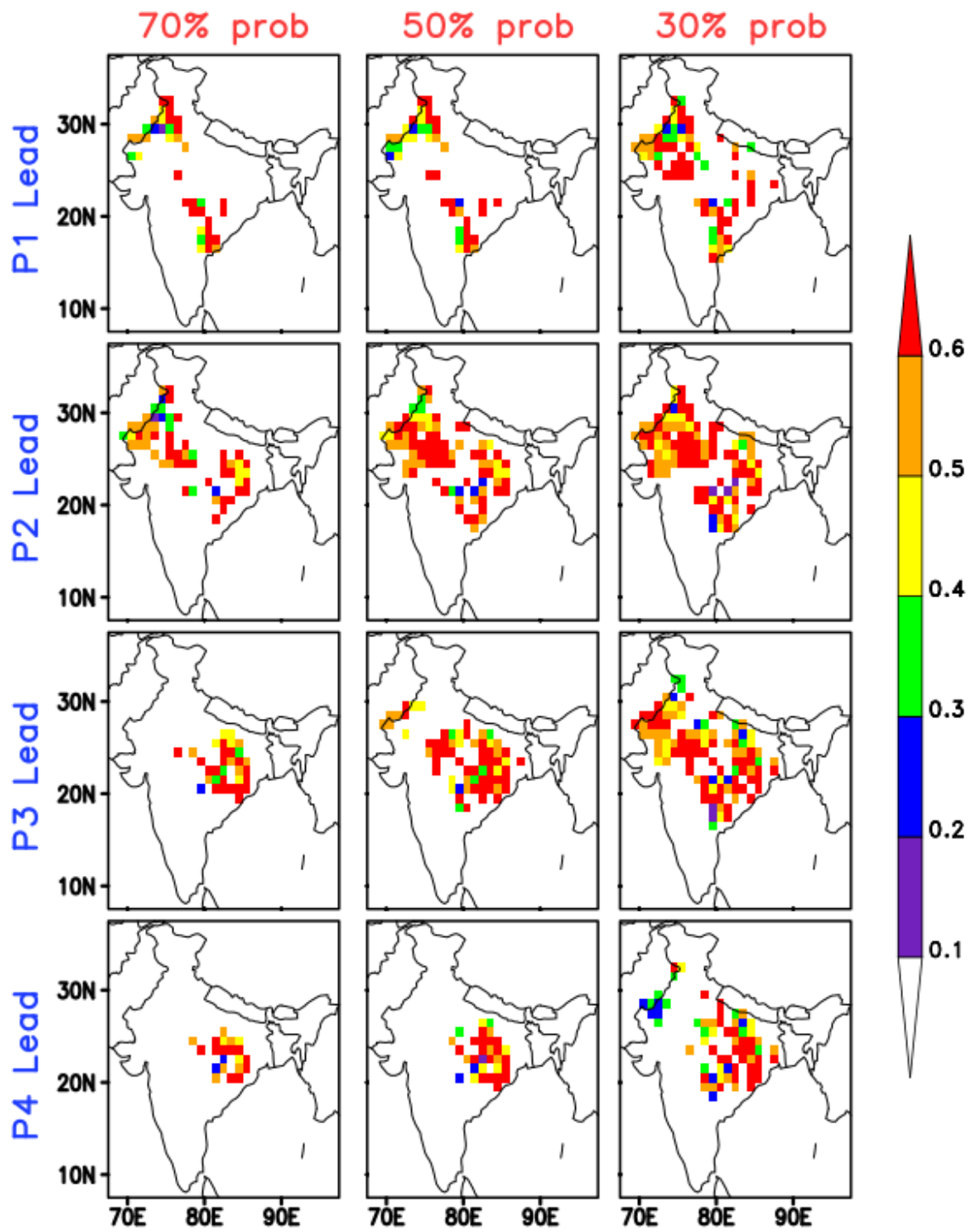


Figure 7: Same as Figure 5, but for SHW category.

15–21 May 2008

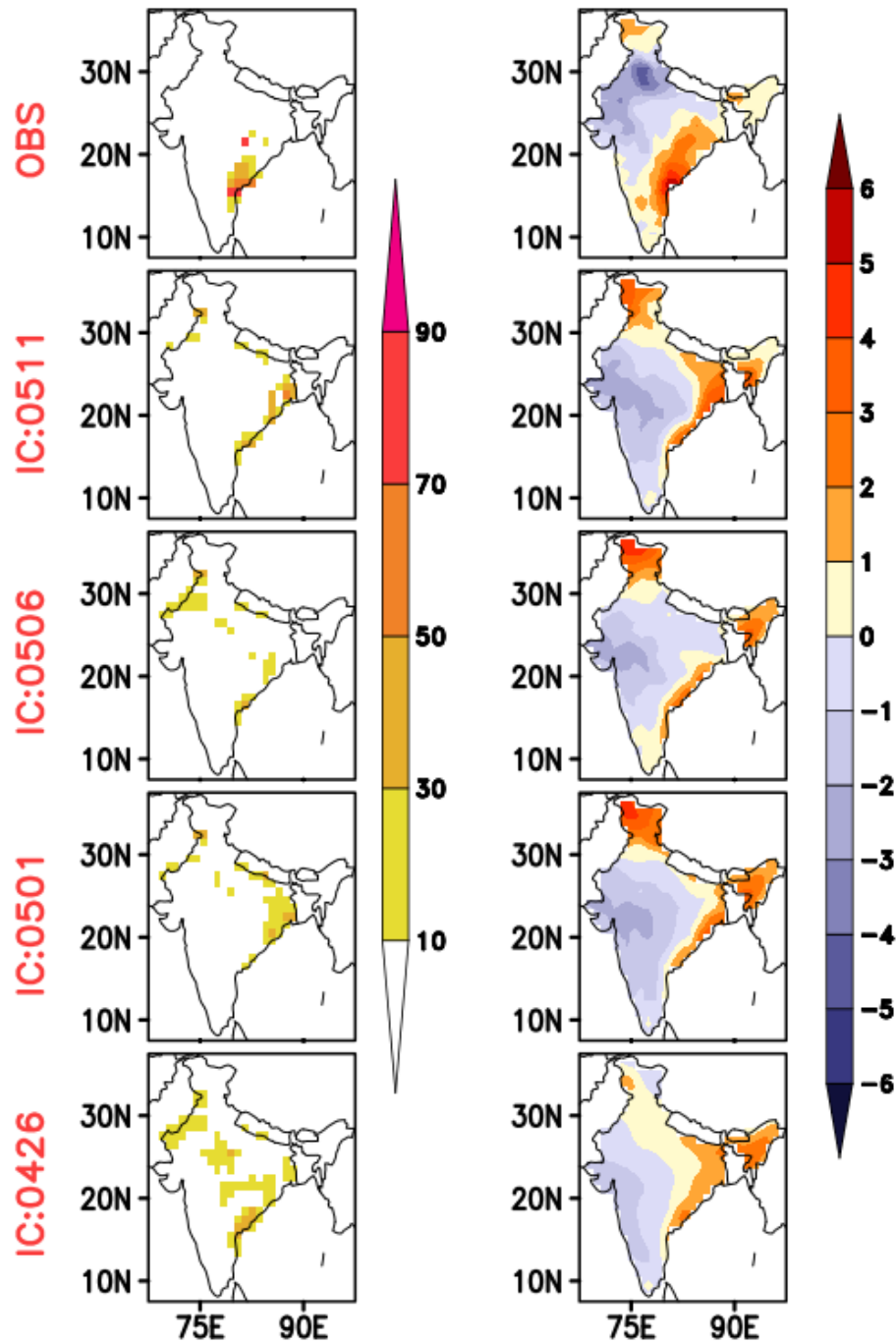


Figure 8: The probability of occurrence of HW event (left column) and the tmax anomalies (right column) during the period 15-21 May 2008 for observation (top panels) and model (subsequent panels).

12May-03Jun 2010

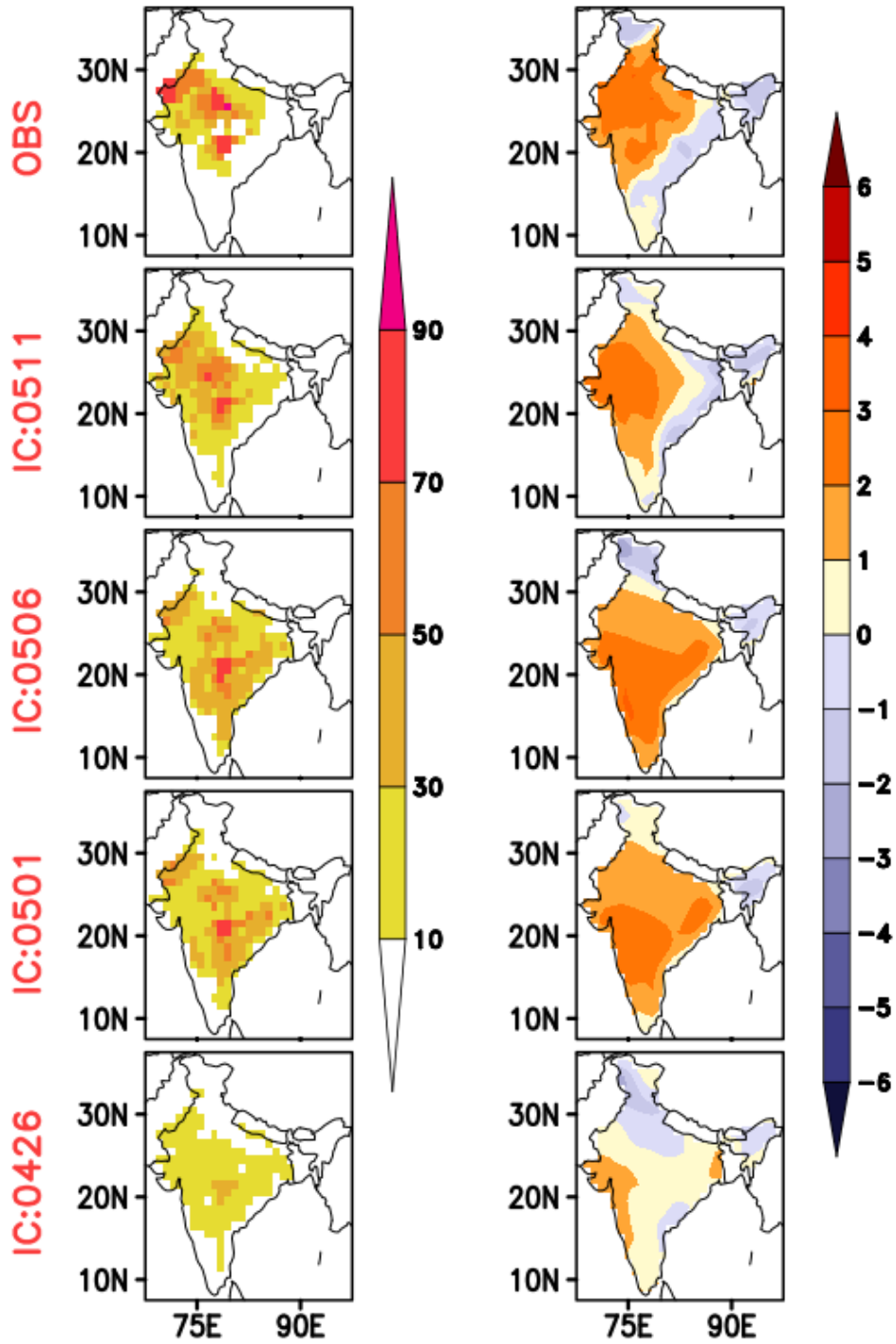


Figure 9: Same as Figure 8, but for the HW during 12 May - 3 June 2010.

02–11Jun 2014

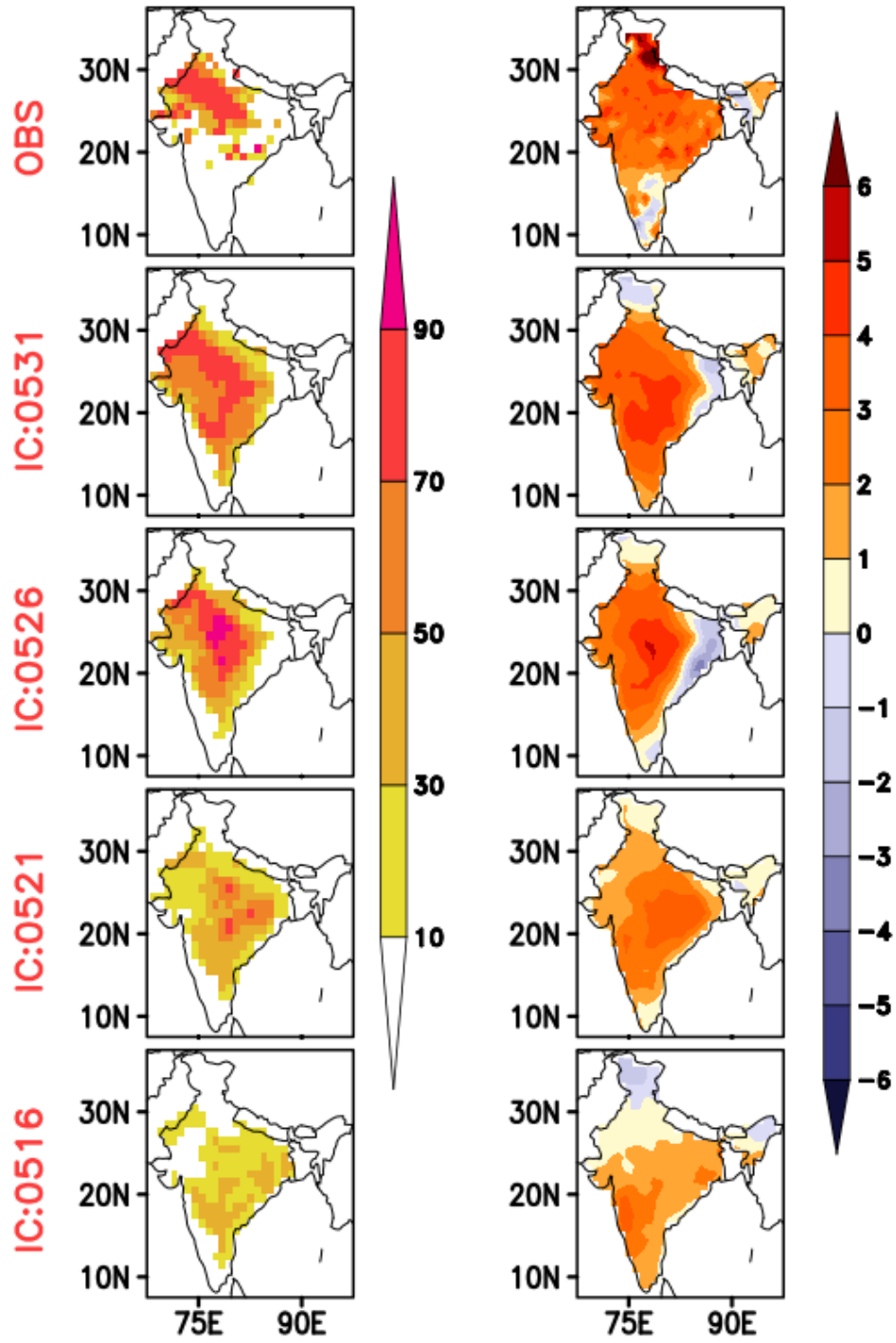


Figure 10: Same as Figure 8, but for the HW during 2-11 June 2014.

18–31 May 2015

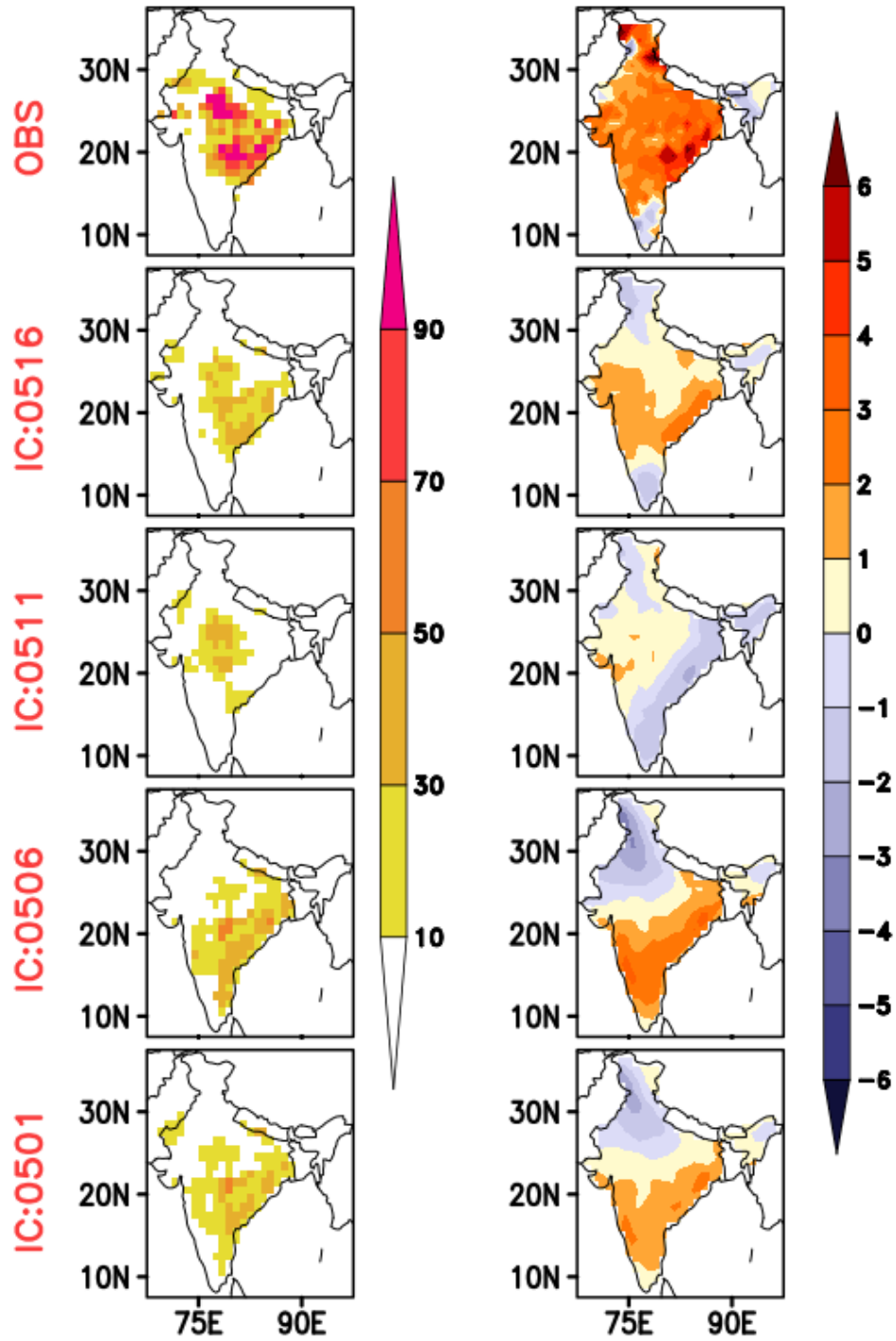


Figure 11: Same as Figure 8, but for the HW during 18-31 May 2015.

19Apr-03May 2016

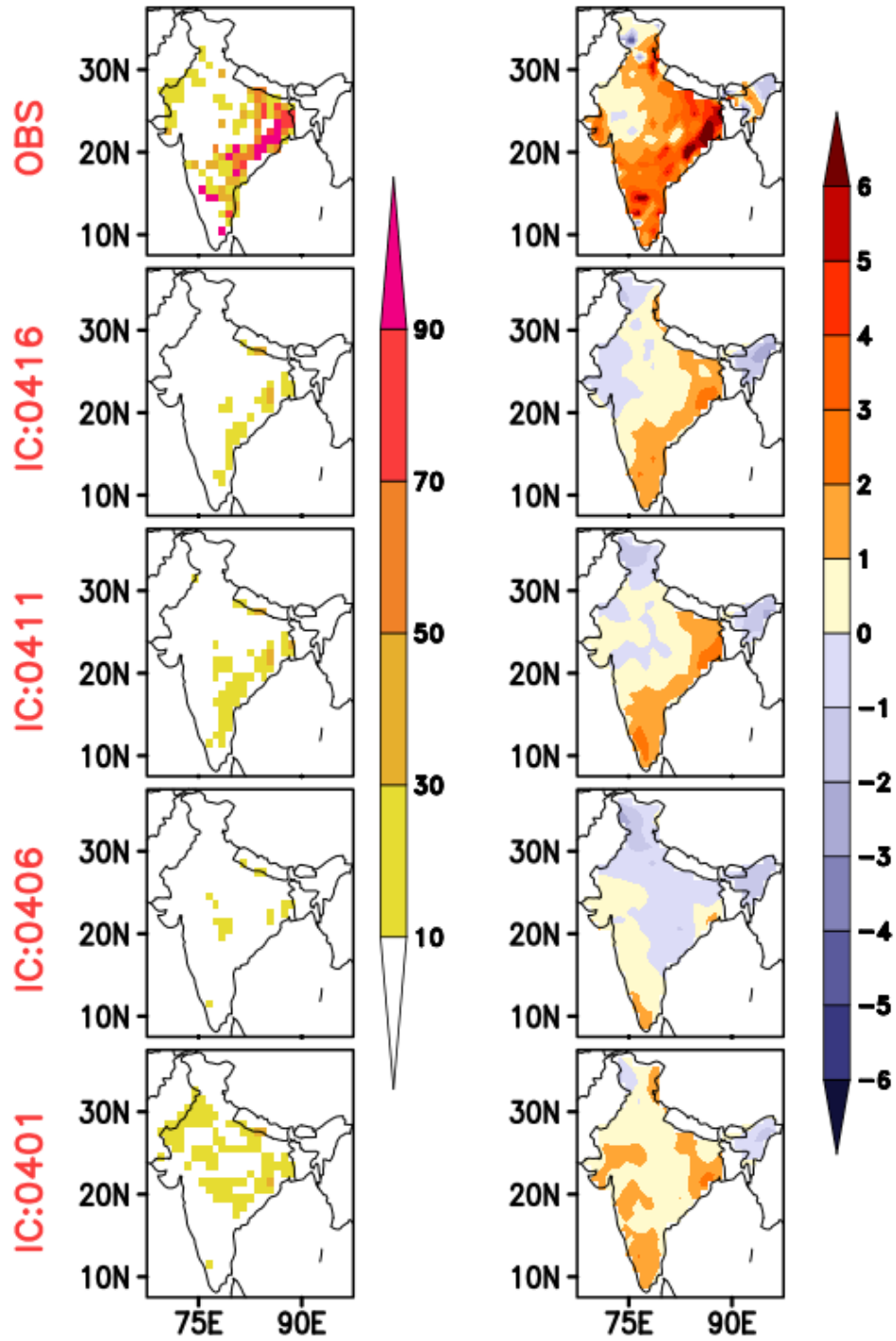


Figure 12: Same as Figure 8, but for the HW during 19 April - 3 May 2016.

12–28May 2016

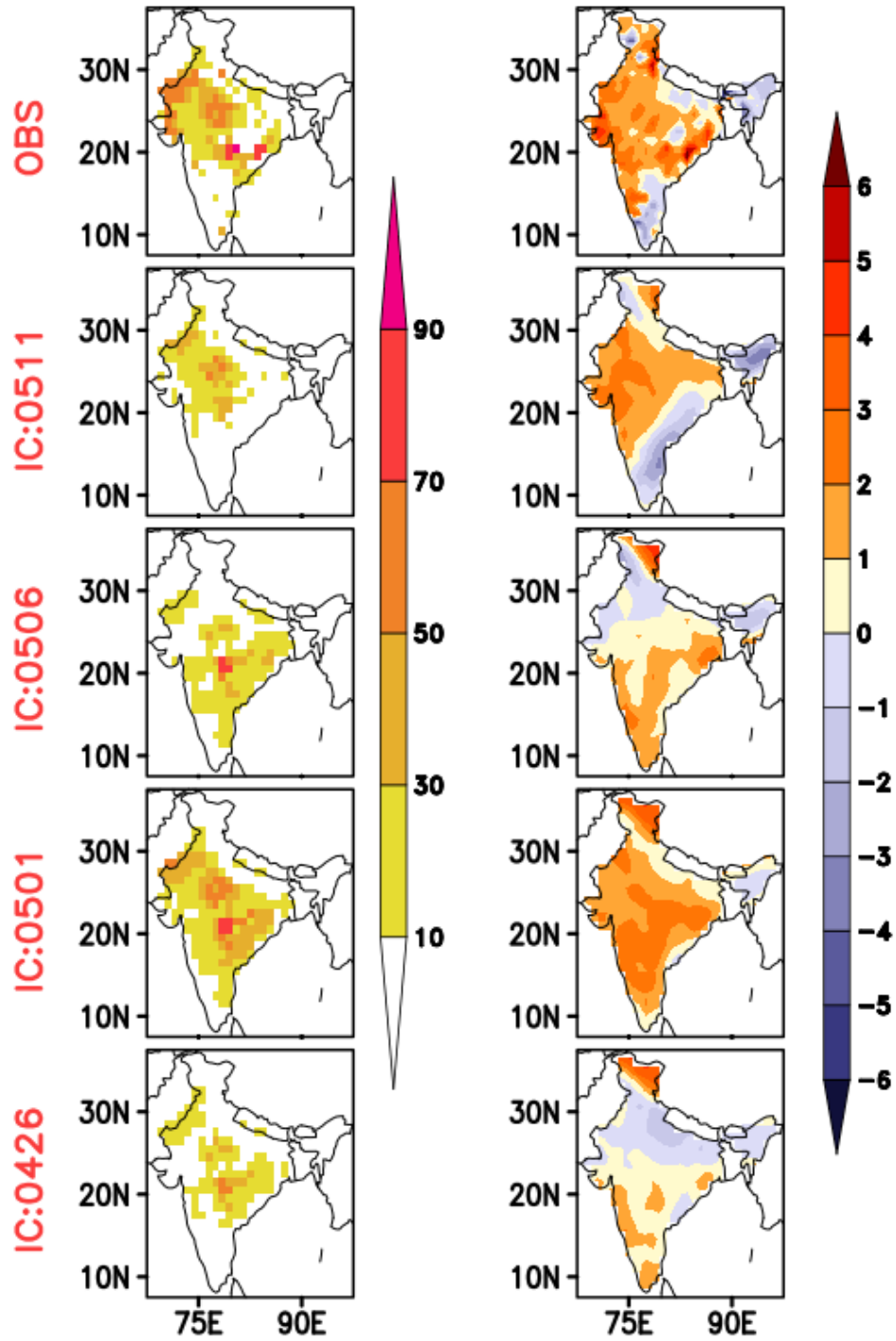


Figure 13: Same as Figure 8, but for the HW during 12-28 May 2016.

03–07 June 2016

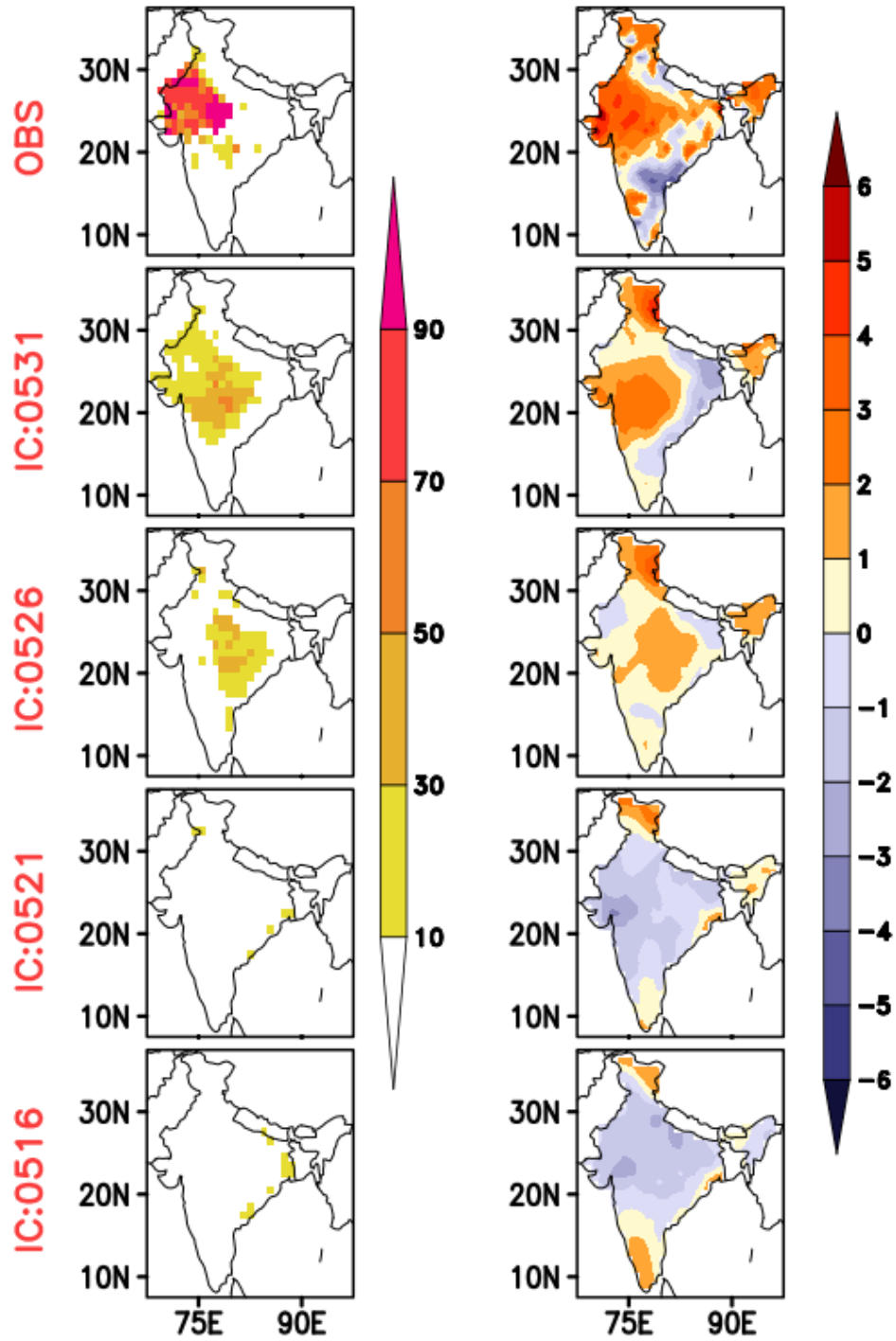


Figure 14: Same as Figure 8, but for the HW during 3-7 June 2016.